Carnegie Institute of Technology
Department of Physics
Pittsburgh 13, Pennsylvania

Office of Naval Research
Contract Nonr 760(05) NR 018-301

Technical Report No. 24

Electronic Specific Heat and Saturation Magnetization of Cr-Fe and Fe-Co Alloys

L. Berger

July 15, 1964

(Submitted by S. A. Friedberg)

Electronic Specific Heat and Saturation Magnetization of Cr-Fe and Fe-Co Alloys*

L. Berger

Carnegie Institute of Technology, Pittsburgh 13, Pennsylvania

Abstract: The collective model of ferromagnetism is applied to various models for the upper third of the 3d band profile of bcc alloys of transition metals. In the first band profile, we consider a rectangular sub-band with rounded lower and upper edges, assuming an intra-atomic exchange integral just large enough to produce ferromagnetism. The low-temperature specific heat coefficient γ is found to have a sharp peak at the electron concentration where ferromagnetism starts (almost empty sub-band), and a deep minimum at the concentration with largest saturation magnetization (half-filled sub-band). This agrees qualitatively with the measurements by Cheng, Wei, and Beck in Cr-Fe and Fe-Co alloys. The agreement becomes quantitative if a second, similar, model of the band profile is used where the density of states inside the sub-band is not constant but drops linearly with increasing energy. The calculated zero-temperature saturation magnetizations agree well with the Slater-Pauling curve for these alloys. In a third model,

---

*Work supported in part by the Office of Naval Research and the National Science Foundation.

the sharp peak of χ is not a simple consequence of the action of the collective model, but reflects the existence of a real peak in the assumed band profile. Then this peak of χ is predicted to happen at an electron concentration slightly larger than the one at which ferromagnetism starts; this seems to be found experimentally in the Cr-Fe series. The calculated saturation magnetizations again agree with the Slater-Pauling curve.

INTRODUCTION

A great wealth of experimental data on the electronic specific heat of body-centered cubic alloys of the first transition series is now available, due to the work of Cheng, Wei, and Beck[1] and of other authors[2-6]. This gives direct information about the profile of the 3d band, at least in the case of alloys where no ferromagnetic spin polarization is present.

The purpose of the present work is to investigate theoretically the effect of a ferromagnetic spin polarization on the low-temperature electronic specific heat of bcc alloys in the framework of the collective approach to ferromagnetism, assuming various models of the band profile. Using the same models, we also compute the zero-temperature saturation magnetizations for these series of alloys, to be compared with the well-known experimental Slater-Pauling curve[7-13]. The present work should also provide a general picture of the electronic structure of the ferromagnetic bcc iron alloys.

It is by comparing the predictions of the collective model with the magnetization data that Slater[7] and Pauling[8] were able to conclude that a region of low density of states should exist in the profile near the Fermi level of chromium. Unfortunately, the value of the magnetization is rather insensitive to the details of the band profile. By combining the specific heat information and the magnetization information, we will see that a more detailed picture of the profile may be obtained.

The calculations are done only in the limit of vanishing temperature, as we think that the collective model of ferromagnetism, in its original form, is not adequate at finite temperatures.

THE COLLECTIVE MODEL OF FERROMAGNETISM

The collective model of ferromagnetism has been discussed by Stoner and by Wohlfarth[14]. We will use a notation similar to that of Wohlfarth[14]. Electrons of a given spin orientation have a density of states $\nu(\epsilon)$, where ϵ is the one-electron energy. The function $\nu(\epsilon)$ is the same for both spin orientations, and is independent of band filling (rigid band approximation). The Fermi level for electrons of spin down is called ϵ_{01}, and that for electrons of spin up is ϵ_{02}. An exchange energy $-J$ is assumed between any two electrons of the same spin orientation; instead of J, used by Lidiard[15], Wohlfarth[14] introduces the parameter θ' defined by $\theta' = NJ/2k$, where k is the Boltzmann constant and N the number of electrons per atom in the band. The energy of the electron system at zero temperature is:

$$E = \int_0^{\epsilon_{01}} \epsilon\,\nu(\epsilon)\,d\epsilon + \int_0^{\epsilon_{02}} \epsilon\,\nu(\epsilon)\,d\epsilon - \frac{J}{2}N_1^2 - \frac{J}{2}N_2^2$$

$$= \int_0^{\epsilon_{01}} \epsilon\,\nu(\epsilon)\,d\epsilon + \int_0^{\epsilon_{02}} \epsilon\,\nu(\epsilon)\,d\epsilon - \frac{J}{2}N^2 + J N_1 N_2 \qquad (1)$$

where N_1 and N_2 are respectively the number of electrons with spin down, and with spin up:

$$N_1 = \int_0^{\epsilon_{01}} \nu(\epsilon)\,d\epsilon \qquad N_2 = \int_0^{\epsilon_{02}} \nu(\epsilon)\,d\epsilon \qquad (2)$$

$$N = N_1 + N_2$$

The condition for an extremal value of the total energy E, under the constraint of constant number of electrons N, may be written:

$$\epsilon_{02} - \epsilon_{01} = J \int_{\epsilon_{01}}^{\epsilon_{02}} \nu(\epsilon)\, d\epsilon \qquad (3)$$

Eq. 3 is the basic equation of the collective model of ferromagnetism in the case of zero temperature. For a given value of N, it always has the paramagnetic solution $\epsilon_{01} = \epsilon_{02}$. If $\nu(\epsilon)$ exceeds the value $\nu_c = 1/J$ at the paramagnetic Fermi level, the paramagnetic solution is unstable, and some ferromagnetic solution will set in, with $\epsilon_{01} < \epsilon_{02}$. We will call ν_c the "critical" density of states. If $\nu(\epsilon) < \nu_c$, the paramagnetic solution is stable; however, a ferromagnetic solution may sometimes still exist even under these conditions, as will be mentioned in a later section.

When ϵ_{01} and ϵ_{02} have been found for a given value of N, by solving Eq. 3, the values of N_1 and N_2 may be calculated by Eq. 2.

The coefficient γ of the low-temperature electronic molar specific heat may be calculated too[16,14]:

$$\gamma = \frac{\pi^2}{3} k^2 N_0 \left(\nu(\epsilon_{01}) + \nu(\epsilon_{02}) \right) \qquad (4)$$

where N_0 is Avogadro's number. This equation is valid only when T is much smaller than the Curie temperature.

The zero-temperature saturation magnetization μ, expressed in Bohr magnetons per atom, is given by:

$$\mu = \frac{g}{2}\left(N_2(\epsilon_{02}) - N_1(\epsilon_{01})\right) \qquad (5)$$

where N_1 and N_2 have been defined by Eq. 2, and where g is the g factor as measured by ferromagnetic resonance[17].

The existence[18] of spin waves in ferromagnetic materials and the persistence[19] of permanent magnetic moments above the Curie point of iron and nickel imply that the collective model of ferromagnetism, in its original form[14], does not describe completely the thermal excitations of a ferromagnet. Therefore, in the present paper we will limit ourselves to the case of vanishing temperature. However, this does not imply that all results of the theory become wrong at finite temperature. In fact, we will see later that the zero-temperature theory does not really require spin alignment in order to apply, but only a spontaneous spin polarization. Some of its results for γ might be valid even above the Curie point of a ferromagnet, provided disordered moments are still present.

We know also that the collective model and the rigid band approximation are concerned only with the electron distribution on the energy scale. They say nothing about the charge density or spin density in space. Therefore, we can predict only certain properties, like the specific heat or the bulk magnetization.

We think that, provided these natural limitations of the collective picture are taken into account, it should apply as well to iron alloys as to nickel alloys, at vanishing temperature. More sophisticated many-body methods[20] are necessary at finite temperature.

APPLICATION TO A RECTANGULAR SUB-BAND WITH ROUNDED EDGES (FIRST BAND PROFILE)

We consider a rectangular sub-band with rounded edges (Fig. 1). We call this very simple model the first band profile. The sub-band is assumed to describe roughly the upper third of the 3d band of bcc alloys, above a region of low density of states located around the Fermi level of chromium. The origin of the energy scale corresponds to the Fermi level of an alloy having $N = 5.3$ el/at.

In the region below the lower edge of the rectangular sub-band, where ferromagnetism is absent, measurements of electronic specific heat[1] (on V-Cr alloys and dilute alloys of iron in chromium) give directly the values of $\nu(\epsilon)$. This experimental information has been used to draw the curve of Fig. 1 for $\epsilon < 0.6$ eV. Similarly, the constant value of $\nu(\epsilon)$ drawn above the top of the 3d band ($\epsilon > 1.25$ eV) has been chosen in such a way as to reproduce correctly the measured electronic specific heat of (fcc) copper[21].

Chromium and its dilute alloys with iron are known to have some kind of an antiferromagnetic spin polarization below room temperature[22]. Because of this complication, one might think that the specific heat measurements do not give directly the band profile in these alloys. However, measurements of specific heat in bcc alloys of the second or the third transition series[23], which are not antiferromagnetic, give a very similar band profile in this range; in particular, there is a low density of states at the Fermi level when $N = 6$ el/at. We will completely ignore the presence of antiferromagnetism in the alloys we consider in the present work.

The shape of the rectangular sub-band itself (Fig. 1) has been chosen arbitrarily. However, it will be shown to lead, when combined with Eq. 3 of the collective model, to a correct prediction of the main features of the electronic specific heat results as measured[1] in series of ferromagnetic Cr-Fe and Fe-Co alloys, and to give values of the saturation magnetization in agreement with the measured Slater-Pauling curve for these alloys.

We have solved Eq. 3 for a few hundreds of values of the electron concentration N. We use the electronic computer, Bendix G-20, at the Carnegie Institute of Technology. We have obtained for each value of N the corresponding values of ϵ_{01}, ϵ_{02}, N_1, N_2, and therefore of γ and μ; they are given by Eq. 2, Eq. 4, Eq. 5. The results for γ and μ are represented by the solid curves of Fig. 2, in the case where $J = 0.294$ eV x at/el . We assume $g = 2.094$, which is the experimental value for pure iron.[17] The γ curve marked "paramagnet" refers to the case $J = 0$, where the alloy would always remain a Pauli paramagnet.

The most striking feature of the theoretical γ curve of Fig. 2 for a ferromagnet is the presence of a sharp peak at the electron concentration at which ferromagnetism starts. It is easy to understand the physical reason for the existence of this peak. If we start filling the 3d band, the alloy is a Pauli paramagnet at first. The two Fermi levels are identical and contribute equal amounts to the density of states. According to Eq. 4, the curve for γ will be simply an image of the band profile, and will rise rapidly when the rectangular sub-band starts filling up at $N = 6.2$ el/at , corresponding to the left side of the peak. However, as soon as the critical density of states necessary for ferromagnetism is reached, the Fermi level ϵ_{01} of the spin down electrons

moves rapidly back below the lower edge of the rectangular sub-band, thereby reducing drastically its contribution to the density of states of the ferromagnet. The value of γ drops therefore rapidly to a fraction of its maximum value, according to Eq. 4, and this corresponds to the right side of the peak.

By many calculations performed with different values of J, we have found that the γ peak is especially prominent if $\nu_c = 1/J$ is only slightly smaller than the maximum density of states reached in the rectangular sub-band. Secondly, the peak is sharp only if the lower edge of the sub-band is not too rounded and if the slope at the edge is large enough. However, if the edge is rounded only very little, and if the slope at the edge is too high, the peak may be so sharp and so narrow as to escape detection. It vanishes completely in the case of an exactly rectangular band.

A similar peak of γ exists at an electron concentration corresponding to almost complete filling of the rectangular sub-band and to the end of the ferromagnetic range. It plays however no role in practice, as no bcc alloy exists in the first transition series with $N > 8.8$ el/at .

Another feature of the theoretical curve of Fig. 2 is a minimum for $N = 8.3$ el/at . The physical reason for this minimum is the following: At this electron concentration, the Fermi level ϵ_{01} is below the lower edge of the sub-band, while the Fermi level ϵ_{02} is above the upper edge. Therefore, the contributions of both Fermi levels to the density of states are very small.

We discuss now the solid curve for the theoretical saturation magnetization μ in Fig. 2. It is made up of two parts. In the first part, μ increases by approximately one Bohr magneton for every electron added to the alloy. The physical reason is that the Fermi level ϵ_{01} of spin

down electrons remains stationary below the lower edge of the sub-band, while ϵ_{02} rises through the sub-band. In the second part of the curve, corresponding to a more than half-filled sub-band, μ decreases approximately by one Bohr magneton for every electron added to the alloy. Here ϵ_{02} remains stationary above the upper edge, while ϵ_{01} rises through the sub-band. The two linear parts of the curve are connected by a rounded region. We notice also, at the left end of the μ curve, a rounded part starting with a vertical (or almost vertical) tangent.

The low-temperature electronic specific heat of bcc V-Cr, Cr-Fe, and Fe-Co alloys has been measured by Cheng, Wei, and Beck.[1] The experimental values of the coefficient γ are plotted as a function of electron concentration in Fig. 2 (see the dashed curve).

A sharp peak is present in the experimental γ curve at $N = 6.4$. This value is close to that at which ferromagnetism starts. Schroder[2,4] has measured the specific heat of some Cr-Fe alloys at elevated temperatures (up to 620°K), in order to investigate further the nature of this peak. The conclusion is that thepeak is really electronic in nature, and is not due to the magnetic anomaly of the specific heat occuring in the neighborhood of the Curie point of a ferromagnet. The Curie point, though falling very rapidly, is in fact still around 50°-80°K in this range[13], that is much higher than the temperature at which the low-temperature measurements have been made. As the curves of C_v/T versus T^2 are reasonably linear at low temperature, it does not seem to us that superparamagnetic clusters[5,6] should play a major role in the peak either.

We see in Fig. 2 qualitative agreement between the experimental results for γ and the predictions of the collective picture as applied to our model of the band. The theoretical curve has a peak of the same

magnitude and the same location, N = 6.4, as the experimental curve. The only descrepancy between theory and experiments exists in the range between N = 7 and N = 8, where theory predicts a plateau for γ ; this question will be discussed in a later section.

The low-temperature saturation magnetization of bcc Cr-Fe alloys has been measured by Fallot[11], and by Nevitt and Aldred[13]. That of bcc Fe-Co alloys has been measured by Weiss and Forrer[10]. These data, converted to Bohr magnetons per atom, are also plotted as a dashed curve in Fig. 2. They constitute a part of the so-called Slater-Pauling curve.[7-9] We see again rather good agreement between theory and experiment. The only descrepancy takes place near N = 8.2, in the Fe-Co alloys corresponding to the largest values of μ. The rounding of the experimental curve is larger than that of the theoretical curve.

To sum up what has been said above, according to this first model the sharp peak of γ observed at N = 6.4 in Cr-Fe alloys is of an electronic nature, but gives only a very distorted image of the true band profile in these alloys. The profile has no sharp sigularities. The existence of the γ peak is rather a consequence of the onset of ferromagnetic spin polarization in a rectangular sub-band with somewhat rounded edges. This peak would be much less prominent, or even completely absent, in bands of other shapes.

This interpretation of the specific heat data is different from that suggested by Cheng, Wei, and Beck[1] themselves, who assume that the data give a direct idea of the true 3d band profile; similarly, Goodenough[24] interprets the peak of γ as representing the true band profile for electrons of e_g symmetry type.

According to our calculation, the Fermi level of spin down electrons in iron (N = 8) is located below the lower edge of the rectangular sub-band. As a result, the density of states at the Fermi level is contributed mostly by spin up electrons, in qualitative agreement with contact potential measurements by Walmsley[25]. This point will be discussed further later.

MODIFICATION OF THE RECTANGULAR SUB-BAND (SECOND BAND PROFILE)

We will now modify the rectangular sub-band of Fig. 1, in order to improve the agreement with experimental γ data. This second band profile is shown in Fig. 3. The modification keeps unchanged the most essential feature of the profile, namely the slight rounding of the edges of the sub-band. However, the density of states, instead of remaining constant inside the sub-band, now decreases linearly with increasing energy.

It becomes then necessary to assume also that the exchange constant J increases gradually with electron concentration. We assume the following relation:

$$J(N) = \frac{1}{2.35 - 0.77\ (N-8)} \qquad (6)$$

This specific expression is such that the density of states (of one spin direction) $\nu(\in)$ at the Fermi level remains always slightly larger than the critical value $\nu_c = 1/J(N)$ while the sub-band is being filled. Otherwise, ferromagnetism would soon stop.

We have solved Eq. 3 of the collective model, with a variable J given by Eq. 6 and assuming the band profile of Fig. 3. The results are shown in Fig. 4, Fig. 5, and Fig. 6. We use the same value $\zeta = 2.094$

as before. These results are very similar to those obtained earlier for the first band profile of Fig. 1 and a constant value of J. The only difference is the disappearance of the plateau of γ for a ferromagnet in the range N = 7 to N = 8 (compare Fig. 2 and Fig. 4). We have now reached a satisfactory fit of the theoretical curves to the experimental data for γ and μ (Fig. 4).

We see that, as in our first calculation, the sharp peak of and the subsequent minimum do not give a true idea of the 3d band profile. The latter is in fact much simpler and smoother than the γ curve.

The motions of the Fermi levels during the filling of the sub-band are represented in Fig. 5. They are very similar to those taking place in the case of the first band profile, which were discussed earlier but not represented graphically.

STUDY OF A SUB-BAND EXHIBITING A PEAK

(THIRD BAND PROFILE)

In the two previous models of the band profile, the sharp peak was due to the action of the collective model of ferromagnetism, rather than to some ad hoc singularity of the band profile itself, which was always very smooth. We shall now investigate a completely different model of the band profile, which exhibits a sharp peak of the density of states. This third band profile is shown in Fig. 7.

The results for γ and μ, as calculated with the collective model of ferromagnetism, are shown in Fig. 8. We have assumed a variable value of J given by:

$$J(N) = \frac{1}{2.2 - 0.5\,(N-8)} \qquad (7)$$

We use the same value $\rho = 2.094$ as before. We reach also here good agreement between theory and experiments for ferromagnetic alloys, as can be seen in Fig. 8.

We have calculated the locations of the two Fermi levels (Fig. 9), and the numbers N_1 and N_2 of electrons of each spin (Fig. 10).

CHOICE BETWEEN THE VARIOUS BAND PROFILES

Of the three band profiles which we have investigated, the first one does not deserve more attention as it is only in qualitative agreement with the experimental data. We will now discuss in more detail the results obtained with the second and with the third band profile, in an effort to decide which one of these two is to be preferred.

Our band profiles may be compared with the electronic specific heat data[23] for bcc alloys of the second or third transition series, which are not ferromagnets but rather Pauli paramagnets. These data should give a direct idea of the correct band profile. No sharp peak is present at $N = 6.4$ in Mo-Re and Mo-Tc alloys. Instead, there is a rounded lower edge very similar to the one we have assumed for our second band profile (Fig. 3). Similarly, measurements of the superconducting transition temperature in these alloys should give some idea of the band profile. There is, again, only a rounded edge and a flat maximum, but no sharp peak, in bcc Mo-Re and W-Re alloys[26] at $N = 6.4$. The same flat maximum has been found[27] in Cr-Re alloys. In all of those alloy series, the bcc range extends only up to approximately $N = 6.5$, so that most of the subband remains out of sight.

Wood[28] has recently done an APW band calculation for bcc paramagnetic iron. The Wood profile has been calculated in more detail through an analytical interpolation procedure by Cornwell and Wohlfarth[29]; it has

some similarities with our band profiles, in particular the existence of a region of low density of states near the Fermi level of chromium, but there are also large differences. For example, the width of the part of the 3d band located above the Fermi level of chromium is at least 2 eV in the case of the Wood profile, and only 1 eV for our second or third profile. Wood's maximum density of states is correspondingly smaller than ours, so much that it cannot account for the γ values observed in Cr-Fe alloys. Moreover, the lower edge of Wood's sub-band exhibits a more complicated structure than the experimental γ data seem to indicate.

Cheng, Wei, and Beck[1] have given a model of the band profile derived from their own specific heat measurements in V-Cr, Cr-Fe, and Fe-Co alloys. It is very similar to our third band profile. However, as their analysis of the data does not take explicitly into account the exchange splittings and their variation with band filling, the minimum of γ present for N = 8.3 appears in their model to be caused by a corresponding minimum of $\nu(\epsilon)$, while it is, in our model, a direct consequence of ferromagnetism.

As was said before, a sharp γ peak has been observed[2,4] even above the Curie points of Cr-Fe alloys. This seems at first to exclude our second band profile as a possible one, since with this profile the γ peak would be due to the existence of ferromagnetism. However, a little reflection shows that a spontaneous spin polarization is required to produce the peak, but not necessarily a spin alignment. Permanent magnetic moments exist[19] in iron above the Curie point, but are disordered. This situation can be described by band theory, as Herring and Kittel[30,31] have shown, if a direction of quantization of the spin is chosen which is

different in each lattice cell, and which is parallel to the local direction of the atomic magnetic moment (direction of the intra-atomic exchange field). The wave-function of a "spin-up" Bloch wave is chosen in such a way that the spin is everywhere parallel to the local quantization direction. The "spin-down" Bloch waves are defined in a corresponding manner. These Bloch waves are approximate eigenfunctions of the hamiltonian, provided the precession period of a spin in the local exchange field is smaller than the time of flight of an electron over a length equal to the range of the short range order of the atomic moments. In the representation of these Bloch waves, the description of the ferromagnet is not very different above and below the Curie point. In particular, the density of states at the Fermi level would not change appreciably. The Fermi level of spin-up electrons would be different from that of spin-down electrons even above the Curie point. We do not know how good this approximation is in the case of ferromagnetic Cr-Fe alloys, but it suggests that the same mechanism by which the collective model of ferromagnetism and the second band profile lead to the existence of a γ peak at low temperature will give the peak even above the Curie point, if disordered permanent magnetic moments are present.

As can be seen in Fig. 2 or Fig. 4, or Fig. 8, the peak of the experimental γ curve is located at a slightly higher electron concentration than the one at which the experimental magnetization curve starts. On the contrary, this shift seems absent in the theoretical curves derived from the second band profile (Fig. 4). We think, however, that the shift might have been present in these curves too, if we had modified very slightly the band profile in such a way as to have the concavity turned upwards in a small region near $\epsilon = 0.65$ eV. The basic idea is that ferromagnetism may start before the critical density of states is reached, provided the concavity is

turned upwards. We do not insist on this point in the present paper, as our numerical calculations have not been done with enough resolution on the electron concentration scale to permit a detailed analysis of the phenomenon. The shift may also be due to another cause, which is discussed below.

High temperature measurements[32,33] of magnetic susceptibility in dilute alloys of iron in chromium seem to indicate the existence of disordered permanent magnetic moments amounting to more than two Bohr magnetons on each iron atom. These alloys are Curie paramagnets at high temperatures, and antiferromagnets below room temperature. Similar paramagnetic moments exist[34] on iron atoms dissolved in molybdenum, homologue of chromium in the second transition series. The saturation magnetization which would be observed in dilute Cr-Fe alloys if these permanent moments could be entirely aligned by a powerful applied field is shown by a dotted straight line on Fig. 2. This spin polarization is probably of a different nature than the one which exists in ferromagnetic Cr-Fe alloys at higher iron concention and which gives rise to the Slater-Pauling curve. It cannot be described within the rigid band approximation. It affects the localized states split off the bottom of the rectangular sub-band by the potential of the iron impurities[34], and not the sub-band itself. Because of a lack of experimental data, it is not yet clear how the dotted magnetization curve of the dilute paramagnetic alloys is to be connected continuously to the solid magnetization curve of the ferromagnetic alloys (Fig. 2). This introduces additional uncertainty into the shape of the left end of the Slater-Pauling curve. According to theory[34] these localized states should vanish when the density of states becomes large, that is when $N > 6.5$. It is quite possible that the presence of these magnetic localized states is the reason why ferromagnetism starts slightly before the sharp γ peak, in the Cr-Fe series.

When the third band profile is used, a shift is obtained automatically in the theoretical results for γ and μ (Fig. 8). The sign of the shift is the same as in the case of the experimental data.

As a conclusion, a part of the available evidence favors the second band profile, and another part the third band profile, and it does not seem possible at the present time to choose between them. This is the reason why we have investigated both of them in detail. We shall discuss in the next section some other evidence about this question, derived from the consideration of the V-Fe alloys and of the Ti-Co-Fe alloys.

It is our opinion that our band profiles are the only ones compatible with the specific heat and magnetization data, in the sense that the real band profile for these alloys should be close to either our second or our third band profile, or lie somewhere in between.

PROPERTIES OF OTHER ALLOYS

LIMITATIONS OF THE PRESENT THEORY

It is known[35,36] that the rigid band approximation, on which the collective model of ferromagnetism rests, is valid when the valences of the two components of the alloy differ by only one or two. Therefore, we can use it on Cr-Fe and Fe-Co alloys. It might apply also to a lesser extent to the V-Fe alloys, for which magnetization[13] and specific data[1] exist. It is not expected, a priori, to work well on the Ti-Co-Fe alloys, for which experimental data exist too[3], as the valence difference is too high.

Another factor is the value of J. The intra-atomic exchange integral is not expected to obey a rigid band model, but rather to depend on an average of the local properties of atoms of the alloy. In particular, it is somewhat doubtful that J would be large enough to cause ferromagnetism in Cr-Fe alloys.

Then, according to our theory, the γ coefficient should follow the curve labeled "paramagnet" in Fig. 4 or Fig. 8, rather than the curve labeled "ferromagnet". The experimental values[1] of γ in the bcc Cr-Mn series seem effectively to rise considerably around N = 6.2 without falling at larger values of N, in agreement with our theory. However, the range of these bcc alloys stops near N = 6.5, so that much uncertainty remains.

The present theory should apply to the bcc Fe-Ni alloys. However, no experimental data on γ are available.

In the case of the V-Fe alloys, a sharp γ peak is observed at N = 5.9 instead of 6.4. It is remarkable that ferromagnetism also starts at N = 5.9 in that series[13]. This tends to show that the existence of the peak is connected to the ferromagnetism, and favors our second model.

A large peak of γ exists at N = 6.4 in ordered Ti-Fe-Co alloys[3]. Even though the rigid band approximation is not expected to apply very well to these alloys, the peak is probably due to the same cause as in the case of the Cr-Fe alloys. Nevitt has not found[37] any measurable magnetization in ordered TiCo(N=6.5) at 7°K. Neutron diffraction[38] failed to show any ordered moments in TiCo at 4°K. These facts seem to show that the γ peak is not associated with the beginning of a ferromagnetic region. Therefore the second of our band profiles seems at first to be ruled out. However, it cannot be excluded that the alloys might have very low Curie points. We repeat here that the second band profile does not really require ferromagnetic alignment above N = 6.4 in order to give the γ peak, but only the existence of permanent atomic magnetic moments due to the polarization of the 3d band. Moreover, according to our theoretical curve based on the second profile (Fig. 4), the average atomic magnetic moments would not be larger than 0.3 Bohr magneton per atom in this region, so that they might be difficult to detect by neutron diffraction even if they were ordered.

A limitation of the present theory is the fact that, as said earlier, we completely neglect the antiferromagnetism of the non-ferromagnetic Cr-Fe alloys. This antiferromagnetism consists probably of a "spin density wave" or of a spiral structure, of the type suggested by Overhauser[39] and Arrott. Such a magnetic structure cannot be described by a simple shift of the Fermi level of spin-up electrons with respect to the one for spin-down electrons. The exchange potential set up by the spin density itself mixes strongly together various Bloch waves of energy close to the Fermi level.

A cusp is present in the experimental γ curve at pure iron (Fig. 2, or Fig. 4, or Fig. 8). Similar cusps exist in the case of other pur metals[40]. They cannot be explained by the rigid band model, and we do not pay further attention to them in the present work.

As noted earlier, our theory predicts that most of the electrons present at the Fermi level of iron have spin up. We find $p = 0.60$ for the second band profile (see Fig. 5) and $p = 0.53$ for the third one (see Fig. 9), where $p = \nu(\epsilon_{02}) - \nu(\epsilon_{01}) / \nu(\epsilon_{02}) + \nu(\epsilon_{01})$. Walmsley[25] finds experimentally $p = 1$, so that the agreement is not quantitative.

CONCLUSIONS

We have found that two different models of the band profile can account in a satisfactory way for the electronic specific heat and magnetization data in Cr-Fe and Fe-Co alloys in the limit of vanishing temperature. In particular, both of them predict correctly the presence of a sharp peak of the electronic specific heat at an electron concentration close to that

where ferromagnetism starts. In the case of one of these models, the sharp peak is not caused by any singularity of the profile, but rather by the motions of the Fermi levels for electrons of both spins. These motions have been investigated with the help of the collective model of ferromagnetism. It is not possible at the present time to decide which of these models is the correct one.

ACKNOWLEDGMENTS

The author would like to thank Prof. S. A. Friedberg for his encouragement in this research, and for many helpful discussions. He is also grateful to Prof. P. A. Flinn and Prof. J. A. Rayne for their critical comments. The Carnegie Institute of Technology Computation Center has provided the computation facilities used in this work.

BIBLIOGRAPHY

1. C. H. Cheng, C. T. Wei, and P. A. Beck, Phys. Rev. 120, 426 (1960).
2. K. Schröder, Phys. Rev. 125, 1209 (1962).
3. L. A. Starke, C. H. Cheng, and P. A. Beck, Phys. Rev., 126, 1746 (1962).
4. K. Schröder, Phys. Rev., 117, 1500 (1960).
5. K. Schröder and C. H. Cheng, J. Appl. Phys., 31, 2154 (1960).
6. K. Schröder, J. Appl. Phys., 32, 880 (1961).
7. J. C. Slater, Phys. Rev., 49, 537, 931 (1936).
8. L. Pauling, Phys. Rev., 54, 899 (1938).
9. W. Shockley, Bell System Tech. J., 18, 645 (1939).
10. P. Weiss and R. Forrer, Ann. phys., 12, 279 (1929).
11. M. Fallot, Ann. phys., 6, 305 (1936).
12. A. Arrott and H. Sato, Bull. Am. Phys. Soc., 3, 42 (1958).
13. M. V. Nevitt and A. T. Aldred, J. Appl. Phys. 34, 463 (1963).
14. E. C. Stoner, J. phys. radium 12, 372 (1951);
    E. P. Wohlfarth, Phil. Mag. 42, 374 (1951).
15. A.B. Lidiard, Proc. Cambridge Phil. Soc., 49, 115 (1953).
16. E. C. Stoner, Proc. Roy. Soc. (London), 169, 339 (1939).
17. A. J. P. Meyer and G. Asch, J. Appl. Phys., 32, 330S (1961).
18. P. E. Tannenwald and R. Weber, Phys. Rev., 121, 715 (1961).
18. J. A. Hofmann, A. Paskin, K. J. Tauer, and R. J. Weiss, J. Phys. Chem. Solids, 1, 45 (1956).
20. D.C. Mattis, Phys. Rev., 132, 2521 (1963).
21. J. G. Daunt, see: C. J. Gorter, Progress in Low Temperature Physics, (North Holland Publishing Company, Amsterdam, 1957) Vol. 1, p. 202.
22. N. S. Rajan, R. K. Waterstrat, and P. A. Beck, J. Appl. Phys., 31, 731 (1960).

23. F. J. Morin and J. P. Maita, Phys. Rev., 129, 1115 (1963).

24. J. B. Goodenough, Phys. Rev. 120, 67 (1960).

25. R. H. Kalmsley, Phys. Rev. Letters, 8, 242 (1962).

26. J. K. Kulm and R. D. Blaugher, Phys. Rev., 123, 1569 (1961).

27. E. Bucher, F. Heiniger, J. Muheim, and J. Muller, Revs. Mod. Phys., 36, 146 (1964).

28. J. H. Wood, Phys. Rev., 126, 517 (1962).

29. L. P. Kohlfarth and J. F. Cornwell, Phys. Rev. Letters, 7, 342 (1961), See also: J. Phys. Soc. Japan, 17, Suppl. B-1, 32 (1962).

30. C. Herring and C. Kittel, Phys. Rev., 81, 869 (1951).

31. C. Herring, Phys. Rev. 87, 60 (1952); 85, 1003 (1952).

32. R. Lingelbach, Z. Physik.Chem. (Frankfurt), 14,1 (1958).

33. M. K. Newman and K. W. H. Stevens, Proc. Phys. Soc. (London),74, 290 (1959).

34. A. M. Clogston, B. T. Matthias, M. Peter, H. J. Williams, E. Corenzwit, and R. C. Sherwood, Phys. Rev., 125, 541 (1962).

35. J. Friedel, Adv. in Physics, 3, 446 (1954).

36. J. C. Slater, article in: Handbuch der Physik, (Springer Verlag, Berlin, 1956), edited by S. Flügge, Vol. 19, p. 81.

37. W. V. Nevitt, J. Appl. Phys., 31, 155 (1960).

38. R. J. Chandross and D. P. Shoemaker, J. Phys. Soc. Japan, 17, Suppl. B-3, 16 (1962).

39. A. W. Overhauser and A. Arrott, Phys. Rev. Letters, 4, 226 (1960).

40. R. Ehrat and D. Rivier, Helv. Phys. Acta, 33, 954 (1960).

CAPTIONS FOR FIGURES

FIG. 1. First model for the upper third of the 3d band of bcc alloys of the first transition series. The horizontal line indicates the value of the "critical" density of states ν_c above which ferromagnetism sets in, assuming $J = 0.294$ eV. x at./el.

FIG. 2. Results of the application of the collective model of ferromagnetism to the band profile of Fig. 1 (first band profile). The coefficient γ of the low-temperature electronic specific heat, and the zero-temperature saturation μ, are plotted as a function of electron concentration, assuming the constant value $J = 0.294$ eV. x at./el. The dashed curves represent the corresponding experimental data for V-Cr, Cr-Fe, and Fe-Co alloys. The dotted line represents the saturation magnetization of localized states split off the lower edge of the sub-band, as deduced from susceptibility measurements on paramagnetic Cr-Fe alloys.

FIG. 3. Second model of the band profile for the upper third of the 3d band of bcc alloys of the first transition series. Compare with Fig. 1.

FIG. 4. Results of the application of the collective model of ferromagnetism to the band profile of Fig. 3 (second band profile). The coefficient γ of the low-temperature electronic specific heat, and the zero-temperature saturation magnetization μ, are

plotted as a function of electron concentration, assuming a variable value of J given by Eq. 6. As in Fig. 2, the dashed curves represent the corresponding experimental data for V-Cr, Cr-Fe, and Fe-Co alloys.

FIG. 5. Fermi level ϵ_{01} of spin-down electrons, and Fermi level ϵ_{02} of spin-up electrons, according to the collective model of ferromagnetism. The second band profile is used, and J is assumed to vary according to Eq. 6. The Fermi level $\epsilon_{01} = \epsilon_{02}$ of a Pauli paramagnet is also represented.

FIG. 6. Number N_1 of spin-down electrons, and number N_2 of spin-up electrons, according to the collective model of ferromagnetism. The second band profile is used, and J is assumed to vary according to Eq. 6. The number $N_1 = N_2$ for a Pauli paramagnet is also represented.

FIG. 7. Third model of the band profile for the upper third of the 3d band of bcc alloys of the first transition series. Compare with Fig. 1 and Fig. 3.

FIG. 8. Results of the application of the collective model of ferromagnetism to the band profile of Fig. 7 (third band profile). The coefficient γ of the low-temperature electronic specific heat, and the zero-temperature saturation magnetization μ,

are plotted as a function of electron concentration, assuming a variable value of J given by Eq. 7. As in Fig. 2 and Fig. 4, the dashed curves represent the corresponding experimental data for V-Cr, Cr-Fe, and Fe-Co alloys.

FIG. 9. Fermi levels ϵ_{01} and ϵ_{02}, in the case of the third band profile. J is given by Eq. 7. The Fermi level $\epsilon_{01} = \epsilon_{02}$ of a Pauli paramagnet is also represented.

FIG. 10. Values of N_1 and N_2, in the case of the third band profile. J is given by Eq. 7. The value of $N_1 = N_2$ for a Pauli paramagnet is also represented.

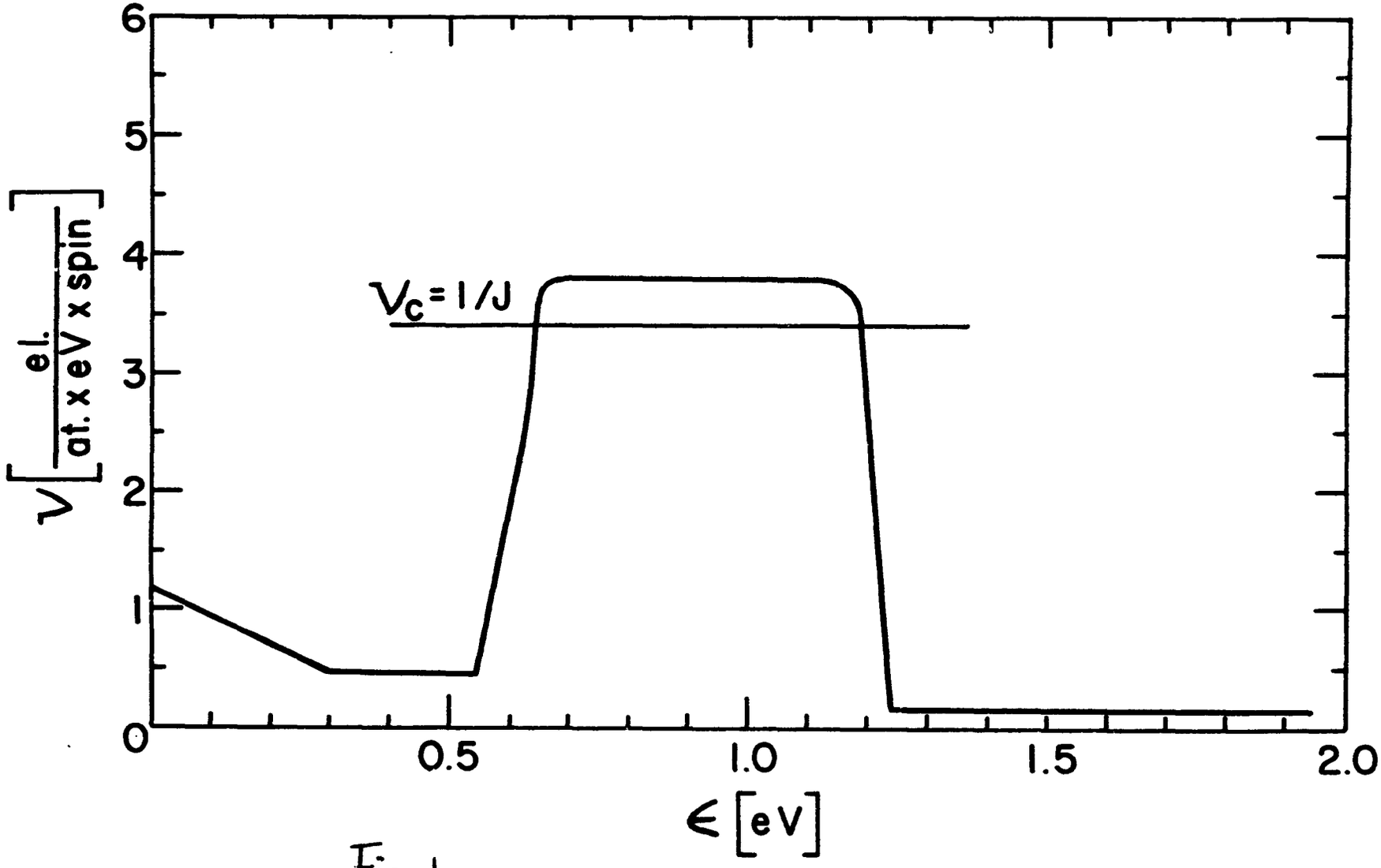
6
5
4
3
2
1
0
0.5
1.0
1.5
2.0
$V_c = 1/J$
$\nu \left[\frac{el.}{at. \times eV \times spin}\right]$
ϵ [eV]

Fig. 1

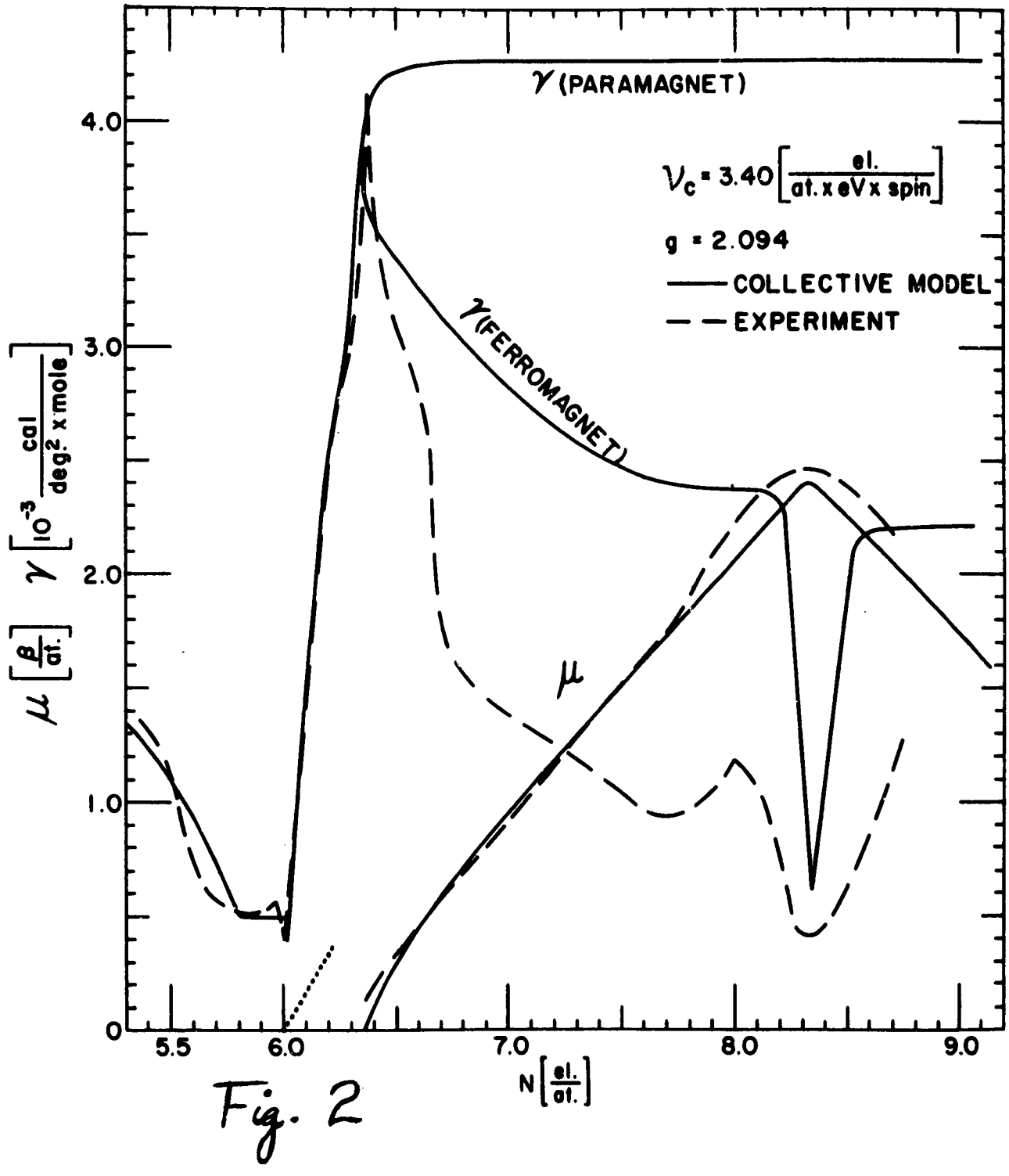
γ (PARAMAGNET)
$\nu_c = 3.40 \left[\frac{el.}{at. \times eV \times spin}\right]$
g = 2.094
COLLECTIVE MODEL
EXPERIMENT
γ (FERROMAGNET)
μ
$\mu \left[\frac{\beta}{at.}\right]$ $\gamma \left[10^{-3} \frac{cal}{deg^2 \times mole}\right]$
4.0
3.0
2.0
1.0
0
5.5
6.0
7.0
8.0
9.0
$N \left[\frac{el.}{at.}\right]$

Fig. 2

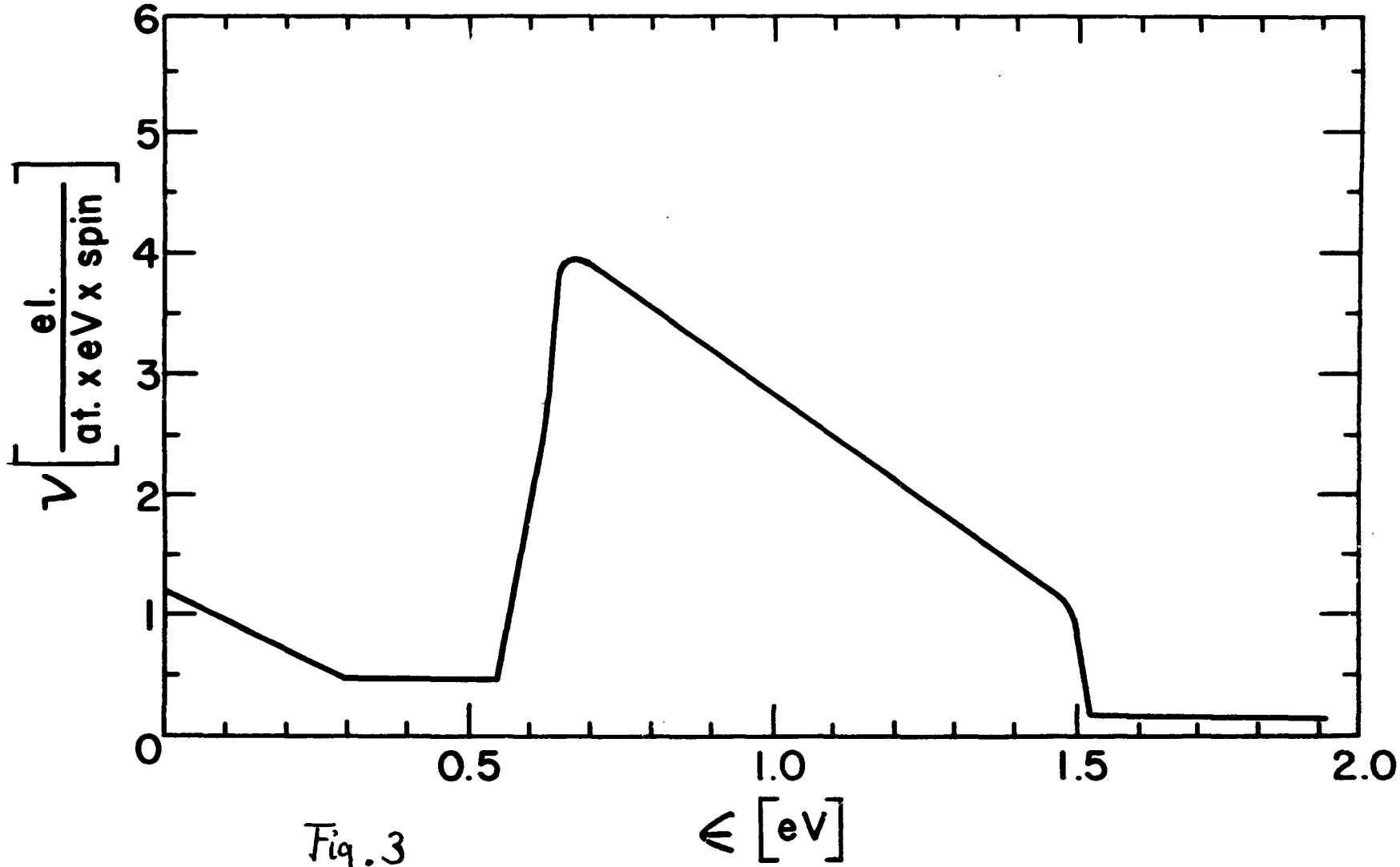

Fig. 3

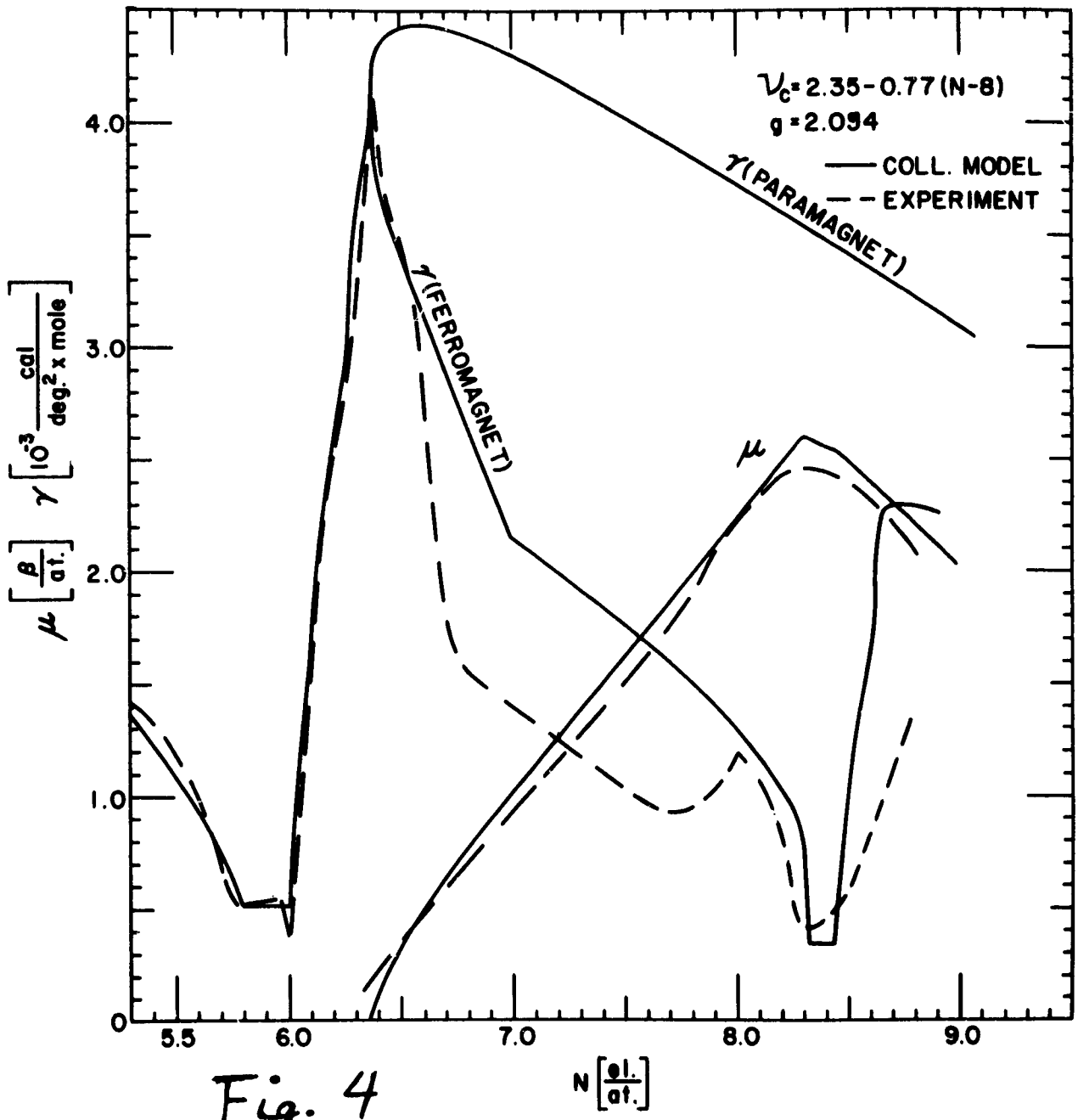
$\nu_c = 2.35 - 0.77(N-8)$
$g = 2.094$
COLL. MODEL
EXPERIMENT
γ(PARAMAGNET)
γ(FERROMAGNET)
μ
$\mu\left[\frac{\beta}{at.}\right]$ $\gamma\left[10^{-3}\frac{cal}{deg.^2 \times mole}\right]$
N $\left[\frac{el.}{at.}\right]$
0
1.0
2.0
3.0
4.0
5.5
6.0
7.0
8.0
9.0

Fig. 4

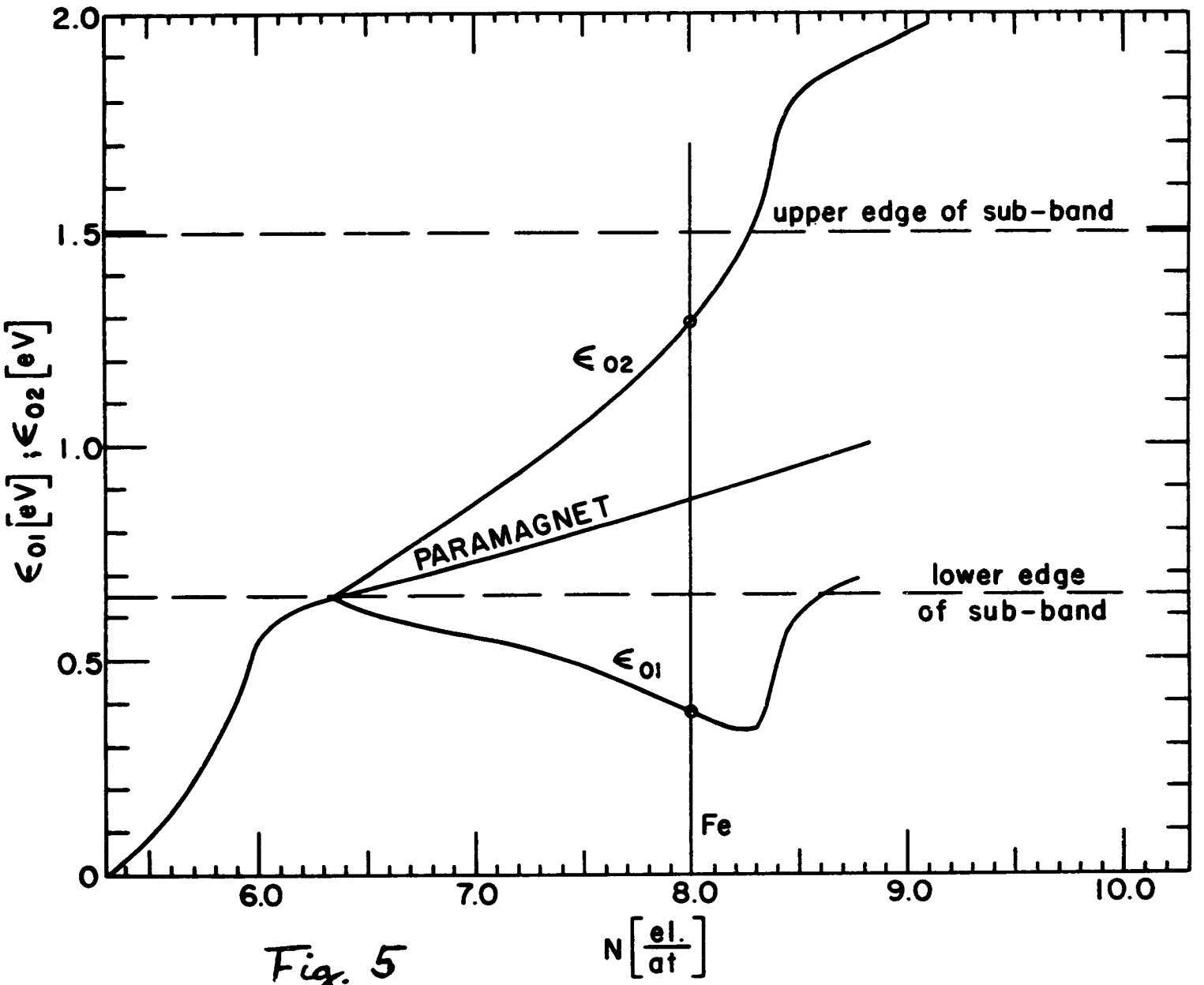
2.0
1.5
1.0
0.5
0
ϵ_{01}[eV] ; ϵ_{02} [eV]
upper edge of sub-band
ϵ_{02}
PARAMAGNET
lower edge
of sub-band
ϵ_{01}
Fe
6.0
7.0
8.0
9.0
10.0
N [el./at]

Fig. 5

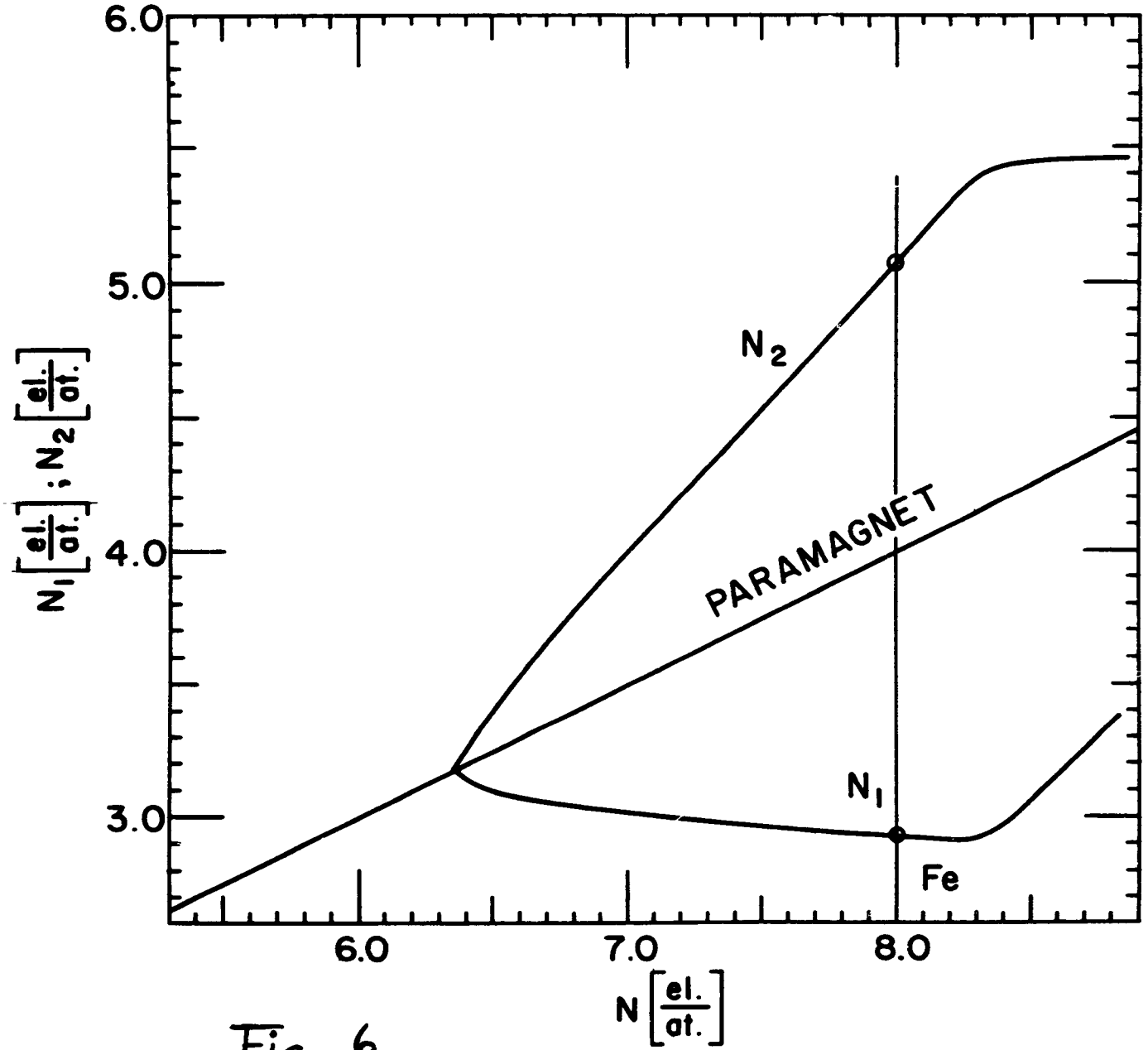
6.0
5.0
4.0
3.0
$N_1\left[\frac{el.}{at.}\right]$; $N_2\left[\frac{el.}{at.}\right]$
N_2
PARAMAGNET
N_1
Fe
6.0
7.0
8.0
$N\left[\frac{el.}{at.}\right]$

Fig. 6

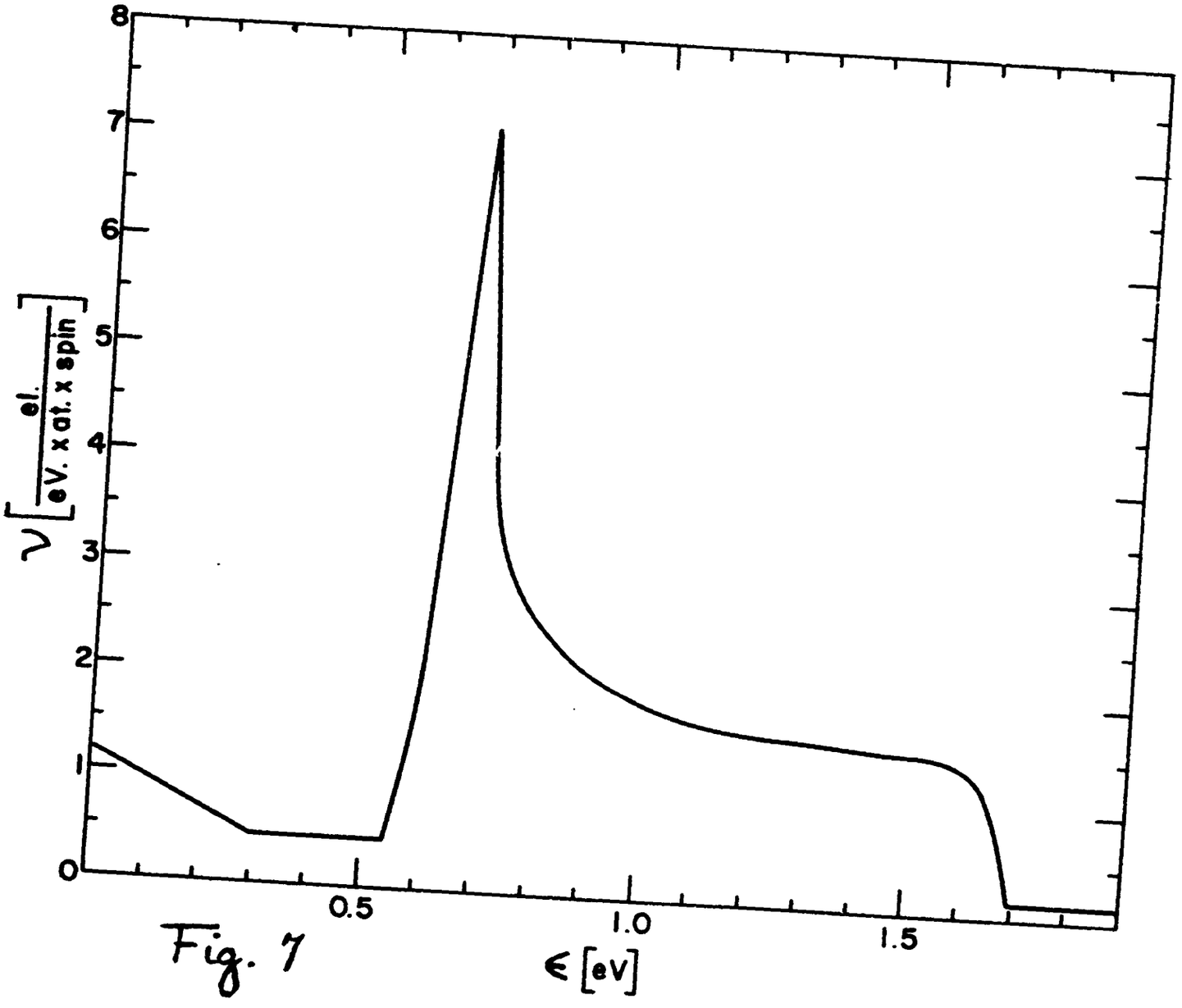

Fig. 7

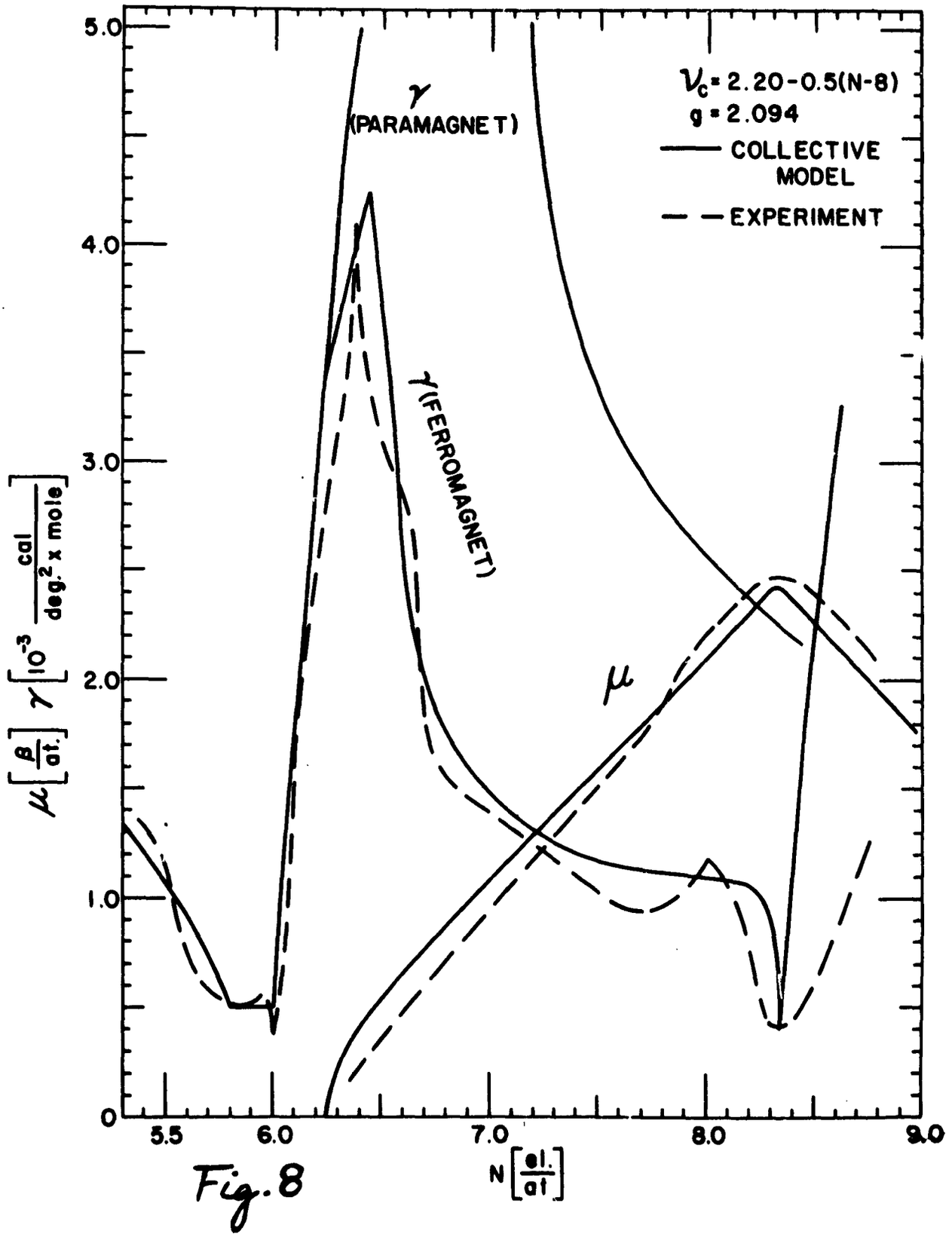
$\nu_c = 2.20 - 0.5(N-8)$
g = 2.094
COLLECTIVE MODEL
EXPERIMENT
γ (PARAMAGNET)
γ (FERROMAGNET)
μ
$\mu\left[\frac{\beta}{at.}\right]$ $\gamma\left[10^{-3}\ \frac{cal}{deg.^2 \times mole}\right]$
$N\left[\frac{el.}{at}\right]$
5.0
4.0
3.0
2.0
1.0
0
5.5
6.0
7.0
8.0
9.0

Fig. 8

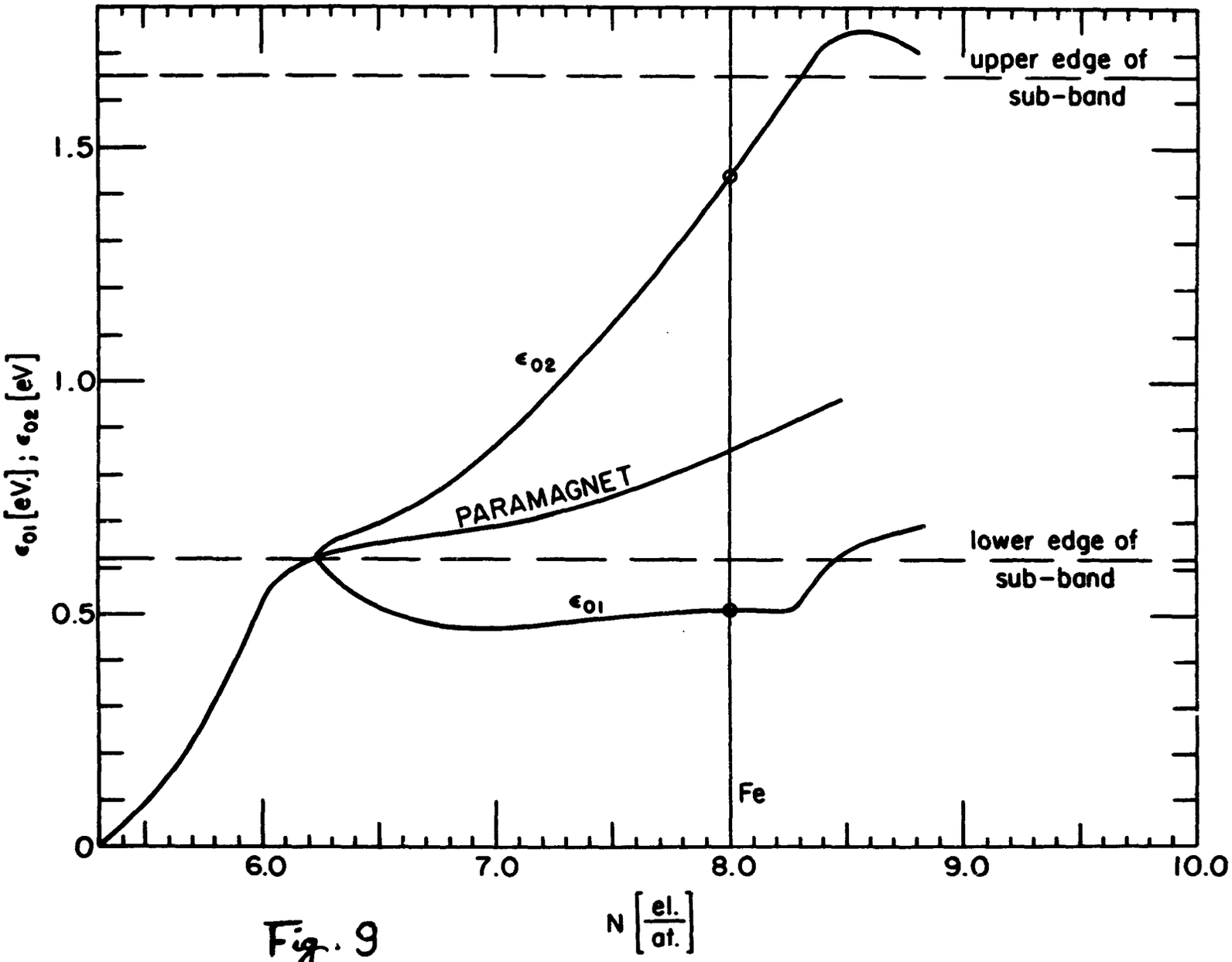
upper edge of sub-band
lower edge of sub-band
PARAMAGNET
ϵ_{02}
ϵ_{01}
Fe
1.5
1.0
0.5
0
6.0
7.0
8.0
9.0
10.0
ϵ_{01} [eV.]; ϵ_{02} [eV]
N $\left[\frac{\text{el.}}{\text{at.}}\right]$

Fig. 9

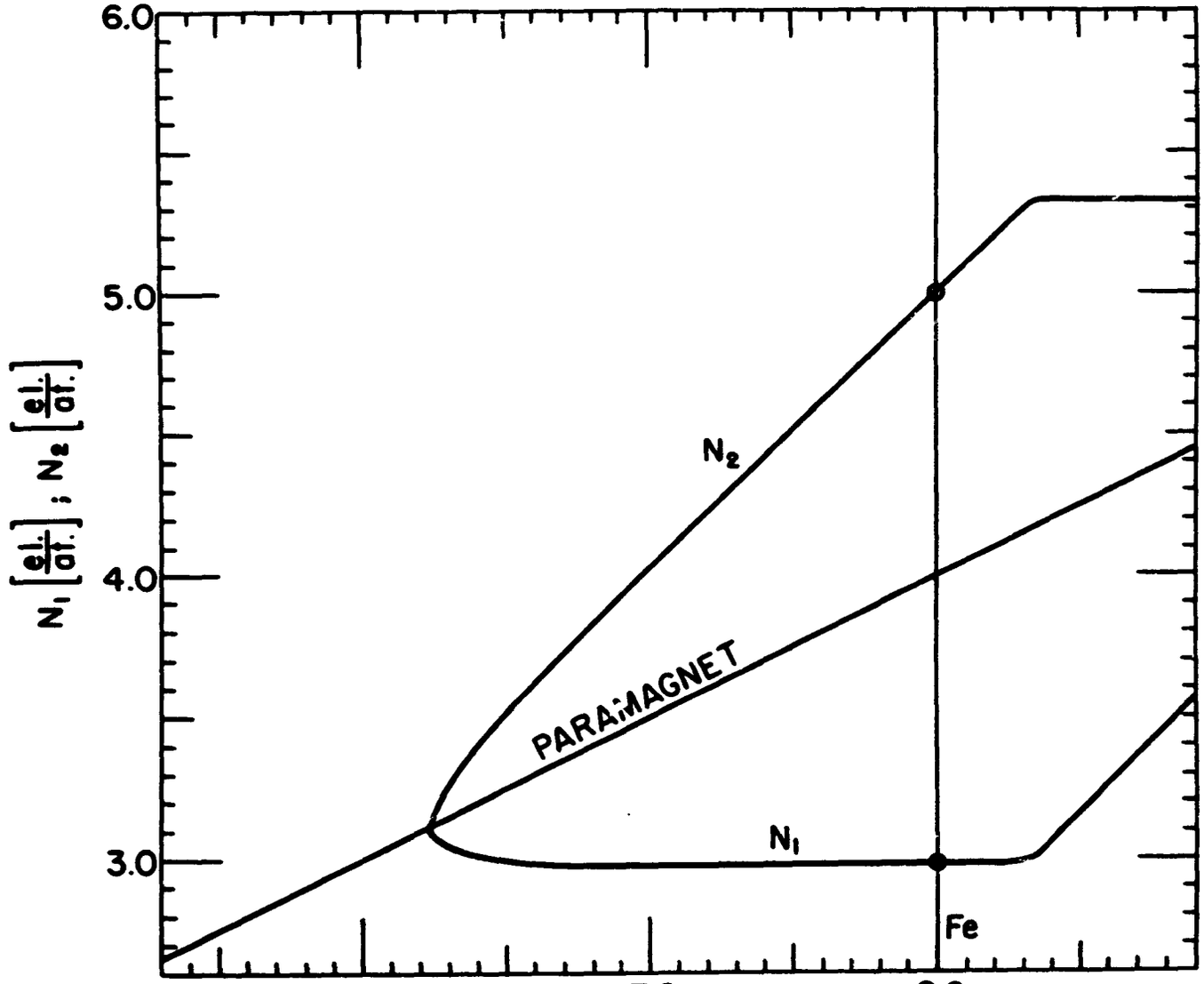
6.0
5.0
4.0
3.0
$N_1\left[\frac{el.}{at.}\right]$; $N_2\left[\frac{el.}{at.}\right]$
N_2
PARAMAGNET
N_1
Fe
6.0
7.0
8.0
$N\left[\frac{el.}{at.}\right]$

Fig. 10